CHEMISTRY
A EUROPEAN JOURNAL

DOI: 10.1002/chem.200600053

FTIR Studies of Iron–Carbonyl Intermediates in Allylic Alcohol Photoisomerization

Thiam Seong Chong, Sze Tat Tan, and Wai Yip Fan*[a]

Abstract: The 532 or 355 nm laser-induced photoisomerization of allylic alcohols to aldehydes catalyzed by $[Fe_3(CO)_{12}]$ or $[Fe(CO)_4PPh_3]$ in hexane was investigated. The Fourier transform infrared (FTIR) absorption spectra of iron–carbonyl intermediate species such as $[Fe(CO)_5]$, $[Fe(CO)_4(R\text{-}C_3H_4OH)]$, and more importantly the π-allyl iron–carbonyl hydride species $[FeH(CO)_3(R\text{-}C_3H_3OH)]$ (R = H, Me, Ph) were recorded during the catalytic process using $[Fe_3(CO)_{12}]$ as the catalytic precursor. When $[Fe(CO)_4PPh_3]$ was photolyzed with 355 nm, $[FeH(CO)_3(R\text{-}C_3H_3OH)]$ was also generated indicating the common occurrence of the species in these two systems. The π-allyl hydride species is long believed to be a key intermediates and its detection here lends support to the π-allyl mechanism of the photoisomerization of allyl alcohols.

Keywords: alcohols · allyl compounds · IR spectroscopy · iron · isomerization

Introduction

Photoisomerization of alkenes by iron–carbonyl species has been the subject of intense study for many years. Several aspects such as the catalytic efficiency of different metal precursors and detection of key intermediates generated separately in low-temperature matrices and in the gas phase have been explored.[1–5] By far, iron–pentacarbonyl ($[Fe(CO)_5]$) has been the precursor of choice for photoisomerization, and in the case of allylic alcohols, aldehydes or aldol products are produced irreversibly upon tautomerization.[6–11] While the proposed active catalyst $[Fe(CO)_3]$ and key intermediate $[FeH(CO)_3(allyl)]$ have been observed mainly under low-temperature matrix or gas-phase conditions[1] and a computational study on the mechanism of iron–carbonyl-mediated isomerization of allylic alcohols to saturated carbonyls has been carried out,[6] more convincing evidence to support the catalytic photoisomerization of allylic alcohols could be obtained if some of these intermediate species could be detected directly during the room-temperature process itself with low catalytic loading.

In this work, we have largely focused on triiron dodecacarbonyl $[Fe_3(CO)_{12}]$ as the catalytic precursor, because of its much milder toxicity as well as the ease of handling the solid. Since the toxic properties of volatile $[Fe(CO)_5]$ could limit its use as a versatile reagent in most organic syntheses, photoisomerization in the presence of $[Fe_3(CO)_{12}]$ at room temperature may offer a better alternative.[4] $[Fe_3(CO)_{12}]$ is also a much less studied catalytic precursor in terms of its mechanism, as it is often assumed to behave in a similar manner to $[Fe(CO)_5]$. Another catalytic percursor, $[Fe(CO)_4PPh_3]$ has also been used in this work for comparison studies.[12]

We have used pulsed laser FTIR absorption spectroscopy to monitor directly the spectral evolution of the precursor, intermediates, and final product of the photoisomerization of allyl alcohols to aldehydes during isomerization. Compared to a broadband source, the intense laser light, either in the visible (532 nm) or UV region (355 nm) could enhance the probability of detecting low concentrations of intermediate species. We have chosen the study of allylic alcohol isomerization rather than that of a simple alkene, because of the ease of monitoring the strong ν_{CO} stretch at 1700–1730 cm^{-1} of aldehyde by using IR spectroscopy. At the same time, transition-metal–carbonyl intermediates produced during the catalytic cycles could be identified by their distinctive CO stretches around 1900–2100 cm^{-1}.

[a] T. S. Chong, S. T. Tan, Dr. W. Y. Fan
Department of Chemistry
National University of Singapore
3 Science Drive 3, 117543 (Singapore)
Fax: (+65) 677-91-691
E-mail: chmfanwy@nus.edu.sg

Supporting information for this article is available on the WWW under http://www.chemeurj.org/ or from the author.

Experimental Section

All the manipulations were carried out in the dark under a nitrogen environment to avoid decomposition of the catalysts. Hexane and toluene were distilled before use and $[Fe(CO)_4PPh_3]$ was prepared according to literature methods.[12] $[Fe_3(CO)_{12}]$ and $[Ru_3(CO)_{12}]$ were obtained from Strem Chemicals, while allyl alcohol, methylallyl alcohol, and phenylallyl alcohol were from Sigma–Aldrich and used without further purification. A typical preparation for each kinetic run would be to mix the allyl alcohol (~0.01 mol) and the metal–carbonyl complex ($\sim 10^{-5}$ mol, loading = 0.1–1.0%) in hexane or toluene (30 mL).

We originally intended to use a broadband xenon lamp source (200 W) to initiate the catalysis, but it was found to be too weak to produce any measurable amount of iron–carbonyl intermediates, although conversion of allyl alcohol to aldehyde was observed. Hence a Nd-YAG pulsed laser system (10 Hz Continuum Surelite III-10, 8 ns pulse width) was used instead to generate either 532 nm (≈10–20 mJ per pulse) or 355 nm (5–15 mJ per pulse) wavelength.

A brief description of the cell used for performing FTIR monitoring on the reaction mixture is given here and can also be found in reference [13]. It wa a home-made stainless steel cell of volume 40 cm^3 fitted with CaF_2 windows for passage of the IR probe beam. Absorbance pathlengths of 0.2 to 5 mm was accommodated by manual adjustment of the window holders. The cell also allowed for placement of quartz or glass windows to permit photodissociation by a laser beam propagated at right angles to the IR probe beam. A magnetic bar was used to provide continuous stirring, while inlet and outlet ports on each side of the cell allowed for N_2 bubbling through the solution if required.

Infrared spectra during irradiation were obtained by using a Nicolet Nexus 870 FTIR spectrometer operating in rapid scan mode (1000–4000 cm^{-1}, 2 cm^{-1} resolution, 16 scans co-added for spectral averaging). Spectral acquisition with the total collection time of 180 min at an interval of 3 min was typically carried out. Difference spectra (solvent, allyl alcohol, and metal precursor as background) were recorded so that the changes in IR absorption with respect to the initial conditions could be observed. Spectral depletion of the reactants was represented by the IR bands pointing in one direction, whereas the production of newly-formed species was shown by the IR bands pointing in the other (as shown in Figure 1). Absolute spectra (only solvent as background) were scanned so that the concentrations of all the detected species could be estimated. In this case, all vibrational bands pointed in the same direction in the spectrum (see Figure 2).

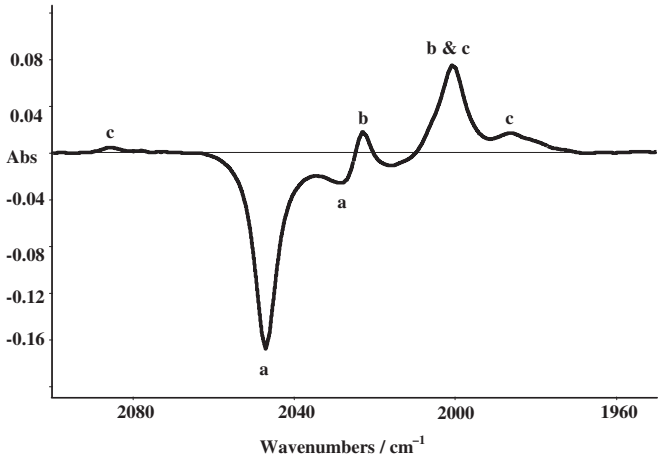

Figure 1. The difference IR bands of a) $[Fe_3(CO)_{12}]$, b) $[Fe(CO)_5]$, and c) $[Fe(CO)_4(C_3H_5OH)]$ during 532 nm irradiation of a solution of $[Fe_3(CO)_{12}]$ (2 mg) and allyl alcohol (1 mL) in hexane (35 mL) after 1 hour.

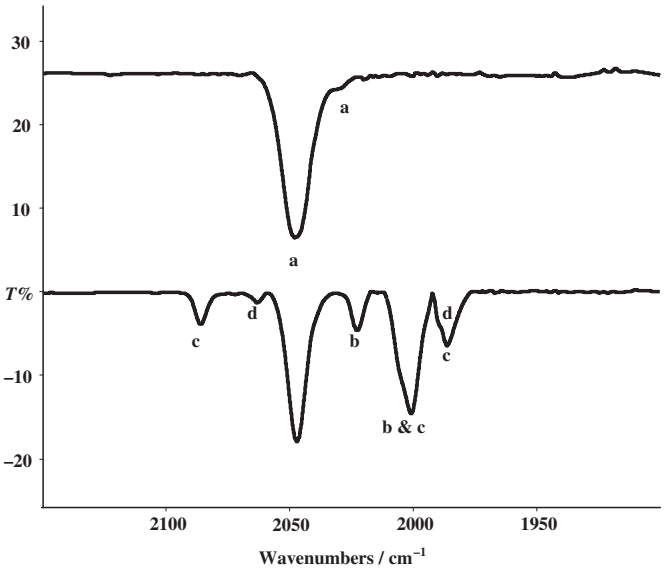

Figure 2. The absolute IR bands of a) $[Fe_3(CO)_{12}]$, b) $[Fe(CO)_5]$, c) $[Fe(CO)_4(C_3H_5OH)]$, and d) $[FeH(CO)_3(C_3H_4OH)]$ during 355 nm irradiation of a solution of $[Fe_3(CO)_{12}]$ (2 mg) and allyl alcohol (1 mL) in hexane (35 mL) after 1 hour.

Beer–Lambert's law (Abs = εcl) was used for concentration determination. The vibrational band extinction coefficients (ε) for the allyl alcohols and aldehydes were determined experimentally in our laboratory by using pure samples of each species as the calibrant. Since most of the iron–carbonyl intermediates here have not been previously detected, we have used the data for the analogous alkene species in which their extinction coefficients of vibrational bands have been determined (Table 1). For example, we used the coefficients for $[Fe(CO)_4(C_3H_6)]$ to estimate the concentration of $[Fe(CO)_4(C_3H_5OH)]$. However, the absolute values of ε are not known for the π-allyl hydride species. As a first approximation, the band intensity was also based on the $[Fe(CO)_4(C_3H_6)]$ for $[FeH(CO)_3(C_3H_4OH)]$ species. Unfortunately the value for the phosphine-substituted species, $[Fe(CO)_3(PPh_3)(C_3H_5OH)]$ was unavailable, hence its concentration could not be estimated. Usually the area under the curve for only one band of each species (the one of least spectral interference from other species) was used for the concentration determination as well as monitoring the progress of the species.

Results and Discussion

$[Fe_3(CO)_{12}]$-catalyzed photoisomerization with 532 nm wavelength laser pulses: The 532 nm photolysis of $[Fe_3(CO)_{12}]$ and allyl alcohol in hexane (35 mL) was first carried out to verify that catalysis was indeed ocurring and to characterize the main transition-metal–carbonyl products formed. Figure 3 (top) shows the concentration profiles of propionaldehyde and allyl alcohol during 532 nm photoisomerization. While the full depletion of $\approx 2\times10^{-5}$ mol mL^{-1} C_3H_5OH was noticeable after one hour of irradiation, only $\approx 1.3\times10^{-5}$ mol mL^{-1} of propionaldehyde was produced under a catalytic loading of 0.5%. This was partly due to the high vapor pressure of aldehyde; a certain amount of it has escaped to fill the volume above the solution within the cell. Other species might have formed, but since the detection of aldehyde in our case was primarily used to verify the

Table 1. Molecular species observed during the photoisomerization of allyl alcohol under various conditions.

Species	Observed IR Bands [cm^{-1}] and selected ε in parenthesis [$mL\,mg^{-1}\,mm^{-1}$][a]	Selected values from reference [1]	
$[Fe_3(CO)_{12}]$	2047 (4.95), 2028		–
$[Fe(CO)_5]$	2022 (4.90), 1999	$[Fe(CO)_5]$	2023, 1996
$[Fe(CO)_4(C_3H_5OH)]$	2085, 2001, 1985(3.57)	$[Fe(CO)_4(C_3H_6)]$	2081, 2000, 1979
$[FeH(CO)_3(C_3H_4OH)]$	2062, 1989	$[FeH(CO)_3(C_3H_5)]$	2064, 1994
$[Fe(CO)_4(Me\text{-}C_3H_4OH)]$	2072, 2013, 1983		–
$[FeH(CO)_3(Me\text{-}C_3H_3OH)]$	2060		–
$[Fe(CO)_4(Ph\text{-}C_3H_4OH)]$	2070, 2011, 1987		–
$[FeH(CO)_3(Ph\text{-}C_3H_4OH)]$	2059, 1987		–
$[Fe(CO)_3(C_3H_5OH)PPh_3]$	2022, 1958, 1930	$[Fe(CO)_3(C_2H_4)PPh_3]$	2022, 1961, 1931
$[Fe(CO)_4PPh_3]$	2051, 1977, 1944	$[Fe(CO)_4PPh_3]$	2052, 1979, 1946
propionaldehyde	1741 (0.40)		–
allyl alcohol	1647 (0.026)		–

[a] The values of ε were assumed to be the same as the alkene iron carbonyl counterparts.

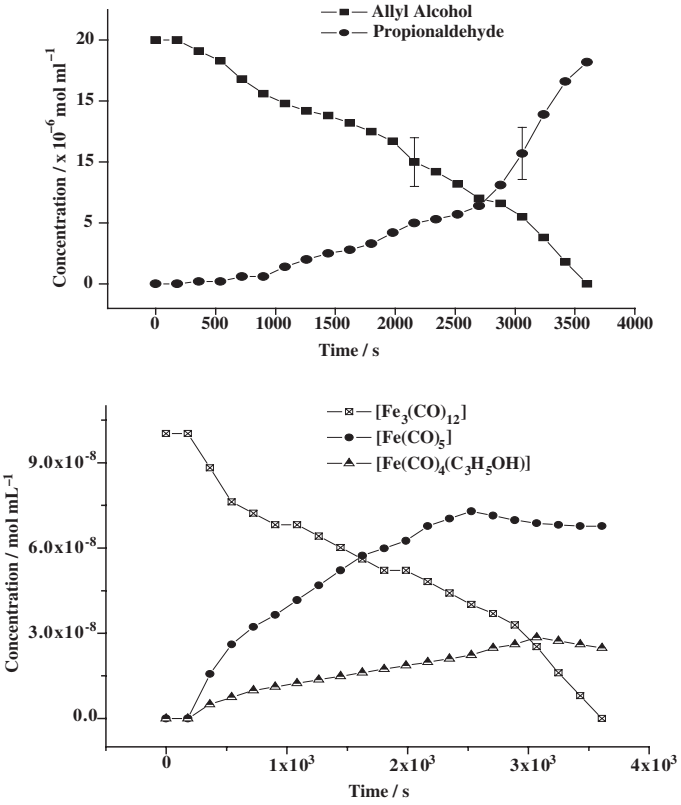

Figure 3. Top: Concentration profiles of propionaldehyde and allyl alcohol during 532 nm photoisomerization of allyl alcohol in hexane with $[Fe_3(CO)_{12}]$. Bottom: Concentration profiles of $[Fe_3(CO)_{12}]$, $[Fe(CO)_5]$, and $[Fe(CO)_4(C_3H_5OH)]$ under the same conditions.

occurrence of catalysis, we did not attempt to detect other products of this system.

Figure 3 (bottom) shows the depletion of $[Fe_3(CO)_{12}]$ and the concurrent production of $[Fe(CO)_5]$ and $[Fe(CO)_4(C_3H_5OH)]$ as the irradiation progressed. The IR bands of $[Fe(CO)_4(C_3H_5OH)]$ species were identified based on the similarity in the band positions with those belonging to $[Fe(CO)_4(alkene)]$ species, such as $[Fe(CO)_4(C_3H_6)]$ (Table 1). The 532 nm irradiation even at higher energies (>20 mJ per pulse) resulted in a slow conversion of $[Fe_3(CO)_{12}]$ to $[Fe(CO)_5]$ and presumably other species including $[Fe(CO)_4]$ and $[Fe(CO)_3]$. Since $[Fe(CO)_5]$ has no absorptions in the green region, the formation of $[Fe(CO)_4(C_3H_5OH)]$ was attributed to the coordination of allyl alcohol with $[Fe(CO)_4]$.[2] The existence of $[Fe(CO)_4]$ in our catalytic system was further supported with the results obtained from visible irradiation of a solution containing $[Fe_3(CO)_{12}]$, allyl alcohol and a trace amount of PPh_3 in hexane, in which $[Fe(CO)_4PPh_3]$ was detected.

From Figure 3 (bottom) the gradual decay of $[Fe_3(CO)_{12}]$ can be seen over the irradiation time. The IR bands of $[Fe(CO)_5]$ were found to evolve faster and achieved three to four times higher concentration than those of $[Fe(CO)_4(C_3H_5OH)]$. By adding the concentration of these two species, we found that $[Fe_3(CO)_{12}]$ mostly dissociated to yield $[Fe(CO)_5]$ and $[Fe(CO)_4(C_3H_5OH)]$ under 532 nm photolysis. We also carried out photoisomerization reactions of other allyl alcohols, such as methylallyl alcohol and phenylallyl alcohol, and similar results were obtained.

Since the aldehyde has been shown to be generated catalytically, the active species should be present in the reaction mixture. As $[Fe(CO)_4(C_3H_5OH)]$ does not absorb in the 532 nm region, it is unlikely that this species will further dissociate to yield $[Fe(CO)_3]$, presumably the active catalytic species.[2,14] However the direct formation of $[Fe(CO)_3]$ from $[Fe_3(CO)_{12}]$ might account for the production of the 16-electron $[Fe(CO)_3(C_3H_5OH)]$ species, which in turn undergoes rapid intramolecular rearrangement to form the 18-electron π-allyl iron hydride species $[FeH(CO)_3(C_3H_4OH)]$ species.[6] Unfortunately we have failed to observe any IR signals attributable to $[FeH(CO)_3(C_3H_4OH)]$. This might be due to the small absorption cross-section of $[Fe_3(CO)_{12}]$ producing only a small amount of intermediate species at each pulse.

$Fe_3(CO)_{12}$-catalyzed photoisomerization with 355 nm wavelength laser pulses: When the rise of the aldehyde signal was compared for the 532 and 355 nm cases, it appeared that under similar experimental conditions the isomerization proceeds about three times faster for the latter case (see Figure 4, top). In addition, a new pair of signals at 2062 and 1989 cm^{-1} (shoulder peak) were observed, which we have assigned to the π-allyl iron carbonyl hydride $[FeH(CO)_3(R\text{-}C_3H_3OH)]$ (Figure 2). The two signals possessed the same spectral evolution as the isomerization progressed, thus supporting their assignment to a single species. IR assignments of the $[FeH(CO)_3(R\text{-}C_3H_3OH)]$ species were also based on the similarity in the IR band positions with those found for $[FeH(CO)_3(C_3H_5)]$ species detected in a matrix as shown in Table 1.[1] As mentioned earlier, the concentration of this

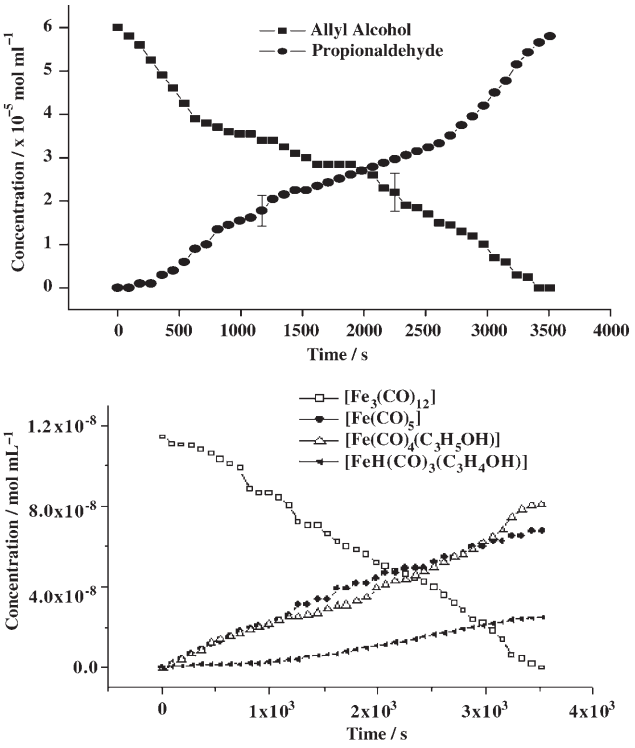

Figure 4. Top: Concentration profile of propionaldehyde and allyl alcohol during 355 nm photoisomerization of allyl alcohol with $[Fe_3(CO)_{12}]$. Bottom: Concentration profiles of $[Fe_3(CO)_{12}]$, $[Fe(CO)_5]$, $[Fe(CO)_4(C_3H_5OH)]$, and $[FeH(CO)_3(C_3H_4OH)]$ under the same conditions.

species was based on the extinction coefficient values derived from $[Fe(CO)_4(C_3H_6)]$. Although the error associated with such an estimate could be large, we believe that this species was indeed present in very low concentrations because of the greater difficulties in its detection with respect to $[Fe(CO)_4(C_3H_5OH)]$. When methylallyl alcohol or phenylallyl alcohol were used as the substrate, the corresponding π-allyl hydrides were also detected, but at lower signal-to-noise ratios. Due to spectral overlap, the lower frequency band of the π-methylallyl hydride species was not observable. Thus subsequent investigations of this species were conducted using the parent allyl alcohol (C_3H_5OH) system itself.

We have also investigated the possibility that the new signals might have come from a bis-allyl alcohol species such as $[Fe_2(CO)_6(C_3H_5OH)_2]$, since its alkene counterpart also possesses two vibrational bands in the same region ($Fe_2(CO)_6(C_3H_6)_2$, 2050, 1975 cm^{-1}).[1] However the intensity of the two detected bands were roughly equal in the spectrum and hence they clearly did not match those of the bis-alkene species, for which the lower frequency vibration is at least ten times more intense than the higher frequency vibration. A detailed search of the literature did not reveal any other matches for the bands observed here. Interestingly, we found that these two bands also occurred in the $[Fe(CO)_4PPh_3]$ catalytic system as will be discussed later.

For the 355 nm irradiation system, a much faster isomerization process was observed primarily due to the larger absorption cross-section of $[Fe_3(CO)_{12}]$, thus yielding more intermediate species to effect the process. $[Fe(CO)_5]$ and $[Fe(CO)_4(C_3H_5OH)]$ have also been detected in this system and unlike visible light irradiation, photodissociation of $[Fe(CO)_5]$ and $[Fe(CO)_4(C_3H_5OH)]$ could now take place upon 355 nm irradiation to produce $[Fe(CO)_3]$ containing species in addition to its direct production from $[Fe_3(CO)_{12}]$.[14] This would provide one of the main factors for the successful detection of $[FeH(CO)_3(R\text{-}C_3H_5OH)]$ at this UV wavelength. Subsequent loss of CO from $[Fe(CO)_4(C_3H_5OH)]$ species upon further 355 nm photolysis might also enhance the production of $[Fe(CO)_3(C_3H_5OH)]$ species, which then rearrange to form more $[FeH(CO)_3(C_3H_4OH)]$ molecules.

Figure 4 (bottom) shows the decay of $[Fe_3(CO)_{12}]$ after 1 hour of 355 nm photolysis, together with the concurrent production of $[Fe(CO)_5]$, $[Fe(CO)_4(C_3H_5OH)]$, and $[FeH(CO)_3(R\text{-}C_3H_5OH)]$. In contrast to the 532 nm case, the concentration of $[Fe(CO)_5]$ was roughly equal to that of $[Fe(CO)_4(C_3H_5OH)]$; this fact indicates that the former species undergoes further photolysis to yield the latter species as one of its main products. However the amount of $[Fe(CO)_4(C_3H_5OH)]$ did not increase indefinitely, since it was also subjected to subsequent photolysis. As expected, the reactive $[FeH(CO)_3(C_3H_4OH)]$ species appeared in lower concentrations, at least three times less, throughout the spectral-monitoring time although its concentration gradually increased during the irradiation period. According to many proposed mechanisms, the π-allyl hydride species comes directly from the intramolecular rearrangement of $[Fe(CO)_3(C_3H_5OH)]$ (isomer **A**, bonded to C=C not directly

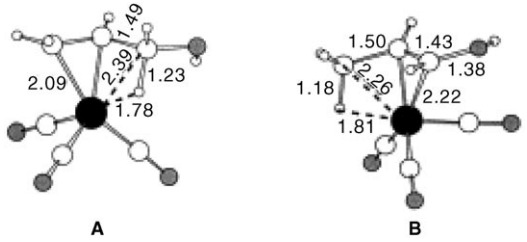

attached to OH), while it decays by means of the reverse process in which the hydride attached to the iron atom transfers back to the allyl alcohol system (isomer **B**, C=C directly bonded to OH); see also Equation (1).

$$[Fe(CO)_3(C_3H_5OH)]\ (\mathbf{A}) \xrightarrow{k_1} HFe(CO)_3(C_3H_4OH) \xrightarrow{k_2} [Fe(CO)_3(C_3H_5OH)]\ (\mathbf{B}) \quad (1)$$

Although it is assumed that the π-allyl hydride species is extremely short-lived, under certain conditions in which $k_2 < k_1$, a buildup of this species could occur that would account for its slight concentration increase towards the later part of photolysis. According to computational models reported in reference [6], the first and second steps of the reaction pos-

sess Gibbs activation energies of $\approx 8\,kcal\,mol^{-1}$ and $\approx 11\,kcal\,mol^{-1}$ respectively. (isomer **A** here is equivalent to structure **2b** and isomer **B** is structure **4a** in reference [6]). This indicates that the conversion of π-allyl hydride to isomer **B** is slightly hindered and thus would have increased its lifetime.

$[Fe(CO)_4PPh_3]$-catalyzed photoisomerization with 355 nm wavelength laser pulses: We have also extended our photoisomerization studies to the $[Fe(CO)_4PPh_3]$-catalyzed system. Figure 5 (top) shows the concentration profiles of the allyl alcohol and aldehyde during 355 nm photoisomerization with $[Fe(CO)_4PPh_3]$ as the catalytic precursor. As expected from previous literature, the catalytic activity was about three to four times less effective compared to those catalyzed by $[Fe_3(CO)_{12}]$ under the same catalytic loading.[2] The photochemistry of $[Fe(CO)_4PPh_3]$ resembles that of $[Fe(CO)_5]$ rather than $[Fe_3(CO)_{12}]$ for which UV light excitation is required for CO-loss activation. A series of possible pathways [Eqs. (2)–(11)] involving detachment of either PPh_3 or CO ligand could be proposed for this system.

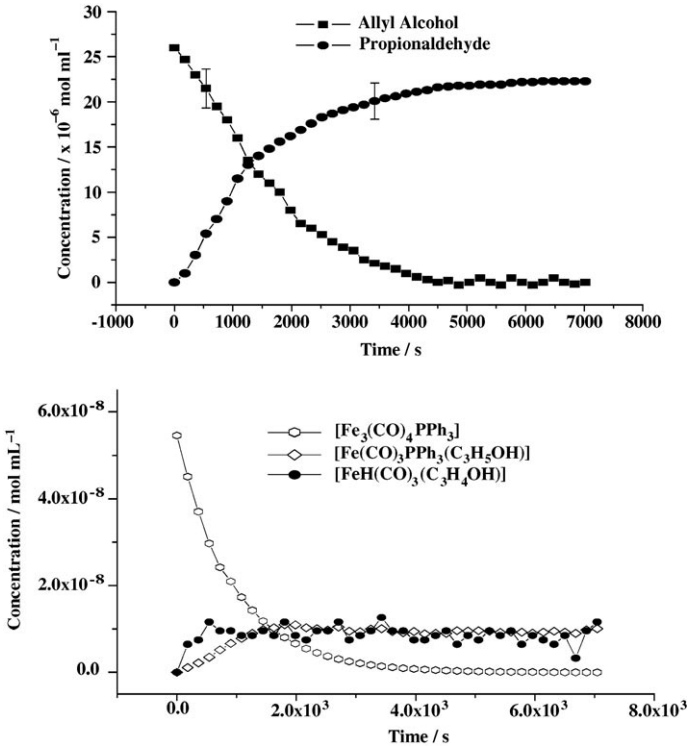

Figure 5. Top: Concentration profiles of propionaldehyde and allyl alcohol during 355 nm photoisomerization of allyl alcohol with $[Fe(CO)_4PPh_3]$. Bottom: Concentration profiles of $[Fe(CO)_4PPh_3]$, $[Fe(CO)_3PPh_3(C_3H_5OH)]$, and $[FeH(CO)_3(C_3H_4OH)]$ under the same conditions. The concentration axis only refers to that of $[Fe(CO)_4PPh_3]$ and $[FeH(CO)_3(C_3H_4OH)]$, since the extinction coefficient of $[Fe(CO)_3PPh_3(C_3H_5OH)]$ is not known.

$$[Fe(CO)_4PPh_3] \xrightarrow{h\nu} [Fe(CO)_3PPh_3] + CO \quad (2)$$

$$[Fe(CO)_4PPh_3] \xrightarrow{h\nu} [Fe(CO)_4] + PPh_3 \quad (3)$$

$$[Fe(CO)_4PPh_3] \xrightarrow{h\nu} [Fe(CO)_3] + CO + PPh_3 \quad (4)$$

$$[Fe(CO)_3PPh_3] + C_3H_5OH \rightarrow [Fe(CO)_3PPh_3(C_3H_5OH)] \quad (5)$$

$$[Fe(CO)_4] + C_3H_5OH \rightarrow [Fe(CO)_4(C_3H_5OH)] \quad (6)$$

$$[Fe(CO)_3PPh_3(C_3H_5OH)] \xrightarrow{h\nu} [FeH(CO)_3(C_3H_4OH)] + PPh_3 \quad (7)$$

$$[Fe(CO)_3PPh_3(C_3H_5OH)] \xrightarrow{h\nu} [FeH(CO)_2PPh_3(C_3H_4OH)] + CO \quad (8)$$

$$[Fe(CO)_4(C_3H_5OH)] \xrightarrow{h\nu} [FeH(CO)_3(C_3H_4OH)] + CO \quad (9)$$

$$[Fe(CO)_3] + C_3H_5OH \rightarrow [Fe(CO)_3(C_3H_5OH)] \quad (10)$$

$$[Fe(CO)_3(C_3H_5OH)] \rightarrow [FeH(CO)_3(C_3H_4OH)] \quad (11)$$

Upon 355 nm photolysis of a hexane solution of $[Fe(CO)_4PPh_3]$ and allyl alcohol, the IR signals due to $[Fe(CO)_3(C_3H_5OH)PPh_3]$ and $[FeH(CO)_3(C_3H_4OH)]$ were observed, as shown in Figure 6. Figure 5 (bottom) shows the concentration profiles of $[Fe(CO)_4PPh_3]$, $[Fe(CO)_3PPh_3(C_3H_5OH)]$, and $[FeH(CO)_3(C_3H_4OH)]$ during the photoisomerization process. Both $[Fe(CO)_3PPh_3(C_3H_5OH)]$ and $[FeH(CO)_3(C_3H_4OH)]$ species were found to be in relatively low concentrations throughout the isomerization process.

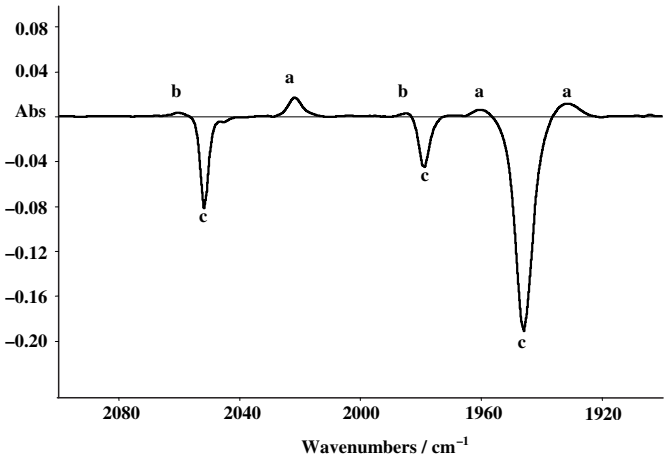

Figure 6. Production of a) $[Fe(CO)_3PPh_3(C_3H_5OH)]$ and b) $[FeH(CO)_3(C_3H_4OH)]$ from 355 nm photolysis of a solution of $[Fe(CO)_4PPh_3]$ (10 mg) and allyl alcohol (1 mL) in hexane (35 mL). Spectrum shown was recorded after 10 min of irradiation.

Attempts were made for the detection of both $[Fe(CO)_4(C_3H_5OH)]$ and $[FeH(CO)_2PPh_3(C_3H_4OH)]$ species, but their vibrational bands were not seen despite changing the allyl alcohol concentrations, increasing the laser energy, or adding free phosphines into the reaction mixture. The detec-

tion of $[Fe(CO)_3PPh_3(C_3H_5OH)]$ species in our experiments suggested that the reaction shown in Equation (5) is preferred over reaction that in Equation (6), and this in turn suggested that the detachment of CO [Eq. (2)] is more likely to occur than the detachment of PPh_3 [Eq. (3)]. However, the sensitivity of FTIR monitoring is not high enough to prove the complete absence of these two reactions [Eqs. (3) and (6)].

At first it seems surprising that we observed the same two vibrational bands attributed to $[FeH(CO)_3(C_3H_4OH)]$ in this phosphine-containing catalytic system. It appears that a common iron allyl hydride species acts as the key intermediate in these two systems. The simplest explanation to account for the formation of $[FeH(CO)_3(C_3H_4OH)]$ is due to the production of $[Fe(CO)_3]$ formed from a direct dissociation of two ligands (CO and PPh_3) from $[Fe(CO)_4PPh_3]$, since the photolysis of $[Fe(CO)_5]$ itself is also known to produce $[Fe(CO)_3]$. If it were the major pathway, it would explain the presence of the hydride species in this phosphine-containing system as well.

However there is an alternate way to consider how the hydride species could be formed. Since $[Fe(CO)_4(C_3H_5OH)]$ was not detected in this system or is present only as a minor component, the possibility of forming $[FeH(CO)_3(C_3H_4OH)]$ from $[Fe(CO)_4(C_3H_5OH)]$ would have to be excluded [Eq. (9)]. The reaction shown in Equation (7), however, remains a possible pathway for generating the hydride species, since $[Fe(CO)_3PPh_3(C_3H_5OH)]$ has been spectrally observed. The release of a bulky group like PPh_3 instead of a CO ligand upon photolysis is quite a common occurrence in metal–phosphine systems as it places less constraint on steric congestion upon intramolecular hydrogen migration.

We have shown that the π-allyl iron carbonyl hydride species $[FeH(CO)_3(C_3H_4OH)]$ is present and most probably takes part in the catalytic cycle for all the three systems investigated here. It was detected directly using FTIR spectroscopy under 355 nm photolysis of $[Fe_3(CO)_{12}]$ and $[Fe(CO)_4PPh_3]$ in the presence of allyl alcohol. Although previous literature reports have indirectly pointed towards the existence of this species by examining the nature of the final products, its direct detection here lends good support to the π-allyl mechanism operating for the isomerization of allyl alcohols as opposed to the metal–hydride addition–elimination mechanism.[8,10]

Acknowledgements

T.S.C. thanks the Institute of Chemical Engineering and Sciences (ICES), ASTAR Singapore for a research scholarship. This work is supported under an NUS grant (143-000-210-112).

[1] J. C. Mitchener, M. S. Wrighton, *J. Am. Chem. Soc.* **1983**, *105*, 1065.
[2] J C. Mitchener, M. S. Wrighton, *J. Am. Chem. Soc.* **1981**, *103*, 975.
[3] A. J. Ouderkirk, P. Wermer, N. L. Schultz, E. Weitz, *J. Am. Chem. Soc.* **1983**, *105*, 3354.
[4] N. Iranpoor, E. Mottaghinejad, *J. Organomet. Chem.* **1992**, *423*, 399.
[5] D. B. Chase, F. J. Weigert, *J. Am. Chem. Soc.* **1981**, *103*, 977.
[6] V. Branchadell, C. Crevisy, R. Gree, *Chem. Eur. J.* **2003**, *9*, 2062.
[7] C. Crevisy, M. Wietrich, V. Le Boulaire, R. Uma, R. Gree, *Tetrahedron Lett.* **2001**, *42*, 395.
[8] R. C. van der Drift, E. Bouwman, E. Drent, *J. Organomet. Chem.* **2002**, *650*, 1.
[9] R. Uma, N. Gouault, C. Crevisy, R. Gree, *Tetrahedron Lett.* **2003**, *44*, 6187.
[10] R. Uma, C. Crevisy, R. Gree, *Chem. Rev.* **2003**, *103*, 27.
[11] H. Cherkaoui, M. Soufiaoui, R. Gree, *Tetrahedron* **2001**, *57*, 2379.
[12] J. L. Graff, R. D. Sanner, M. S. Wrighton, *Organometallics* **1982**, *1*, 837.
[13] T. S Chong, P. Li, W. K. Leong, W. Y. Fan, *J. Organomet. Chem.* **2005**, *690*, 4132.
[14] P. Portius, J. Yang, X. Sun, D. C. Grills, P. Matousek, A. W. Parker, M. Towrie, M. W. George, *J. Am. Chem. Soc.* **2004**, *126*, 10713.

Received: January 14, 2006
Published online: April 27, 2006

